The effect of Y_2O_3 and $YFeO_3$ additions on the critical current density of YBCO coated conductors

2014 J. Phys.: Conf. Ser. 507 022012

(http://iopscience.iop.org/1742-6596/507/2/022012)

Journal of Physics: Conference Series **507** (2014) 022012 doi:10.1088/1742-6596/507/2/022012

The effect of Y_2O_3 and $YFeO_3$ additions on the critical current density of YBCO coated conductors

M Lao,[1] M Eisterer,[1] O Stadel,[2] A Meledin,[3] G van Tendeloo[3]

[1]Atominstitut, Vienna University of Technology, Stadionallee 2, 1020, Vienna, Austria
[2]PerCoTech AG, Bienroder Weg 53, 38108 Braunschweig, Germany
[3]EMAT Research Group, University of Antwerp, Groenenborgerlaan 171, B-2020, Antwerp, Belgium

E-mail: mlao@ati.ac.at

Abstract.
The pinning mechanism of MOCVD-grown YBCO coated conductors with Y_2O_3 precipitates was investigated by angle-resolved transport measurement of J_c in a wide range of temperature and magnetic fields. Aside from the Y_2O_3 nanoprecipitates, a-axis grains and threading dislocation along the c-axis were found in the YBCO layer. The Y_2O_3 precipitates are less effective pinning centers at lower temperature. The tapes with precipitates show a higher anisotropy with larger J_c at $H \parallel ab$ than $H \parallel c$. This behavior was attributed to the preferred alignment of the nanoprecipitates along the ab-plane.

1. Introduction

The second generation high-temperature superconducting wire based on YBCO ($YBa_2Cu_3O_{7-\delta}$) grown-epitaxially on metallic substrates has shown a great promise for high-current transmission applications. The presence of vortex pinning sites either in the form of dislocations, twin boundaries, stacking faults or the addition of artificial pinning centers such as nanoprecipitates and columnar defects was shown to greatly enhance J_c especially at high magnetic fields. The addition of random pinning centers has attracted much attention since they are sources of isotropic pinning in the superconductor. One of the most common forms of random pinning center are Y_2O_3 precipitates which greatly enhance J_c of YBCO tapes [1, 2, 3, 4]. Some studies explored the effect of adding magnetic nanoparticles such as $YFeO_3$ that also enhanced J_c without degrading the superconducting characteristics of the films [5]. Another important aspect is the deposition process for the production of YBCO coated conductors, such as pulsed laser deposition (PLD), chemical solution deposition (CSD) and metal-organic chemical vapor deposition (MOCVD). Each deposition process leads to a particular formation of pinning centers which cause variations in the behavior of J_c at different temperatures and fields. The actual effects of the nanoprecipitates and correlated defects formed through these deposition processes are still to be determined in a broader range of temperatures and fields.

The MOCVD technique offers a high potential for large-scale production of superconducting tapes. The cheapest possible way to produce high-efficiency wires has to be found. A combination of the MOCVD and CSD approach to grow YBCO and oxide buffer layers on textured metal substrates such as NiW is one of the low-cost alternatives to high-vacuum deposition techniques [6].

In this study, the effect of Y-based precipitates on J_c of MOCVD-grown YBCO on a MOCVD (Y,Ce)$O_{1.5+x}$ and CSD-grown $La_2Zr_2O_7$ (LZO) buffer layer on a magnetic Ni5%W substrate will be investigated. The microstructure formed in the superconducting layer will be related to angle-resolved measurements of J_c at fields up to 5 T and temperatures down to 20 K to provide a more concise view of the pinning contributions in these specific tapes.

2. Experimental details

The oxide buffer layer (Y,Ce)$O_{1.5+x}$ and YBCO layer were grown via a MOCVD reel-to-reel system in PerCoTech [10] on a Ni5%W substrate with a 140 nm CSD-grown LZO buffer layer. The YBCO layer of the first tape was deposited in two-pass process to form a total thickness of 700 nm. A 10 mol% of Y_2O_3 was added to the second tape and the third tape contains 1 mol% of $YFeO_3$. Both tapes were grown in a single-pass process. The estimation of the $YFeO_3$ and Y_2O_3 additions are based on the Fe and Y content in the precursor solution. The tapes will be denoted as YBCO, YO and YFO, respectively. The critical temperature of the YFO tape was found to be 1.3 K lower than YBCO which indicates that iron was incorporated in the superconducting layer. The characteristics of the tapes are summarized in Table 1. All the tapes have a width of 10 mm.

Table 1. Summary of the PerCoTech tape characteristics.

Name	Addition	Thickness (nm)	$T_{c,onset}$ (K)	I_c (A), 77 K 10mm-width	Bridge dimension (mm^2)
YBCO	-	700	90.5	85	0.45 × 2.40
YO	10 mol% Y_2O_3	380	89.7	48	0.65 × 3.25
YFO	1 mol% $YFeO_3$	450	89.2	47	0.55 × 3.65

Bridges were patterned on the tapes for measurements at lower temperature. The dimensions are given in Table 1. Transport measurements were made at magnetic fields of up to 5 T. The measurements at 77 K were made with the 10-mm tapes and the bridged tapes were used for measurements at temperatures from 55 K down to 20 K. The four-probe method was used with 1 μV cm^{-1} criterion. All J_c-anisotropy measurements were made under maximum Lorentz force configuration.

The microstructure of the tape with $YFeO_3$ addition was investigated by TEM using a FEI Tecnai G2 electron microscope operated at 200 kV, a Philips CM30 electron microscope operated at 300 kV and a FEI Titan electron microscope operated at 120, 200 and 300 kV.

3. Results and Discussion

The self-field J_c of the three tapes is 1.21, 1.26 and 1.04 MA cm^{-2} for the YBCO, YO and YFO tape, respectively. Figure 1a shows angle-resolved measurements of J_c at 77 K for the YBCO tape which shares a similar behavior with the other two tapes. An *ab*-peak is observed and a small *c*-axis peak appears at intermediate fields. Comparing the $J_c(\theta)$ of the three tapes in figure 1b, the YO tape has the highest J_c along $H \parallel ab$ followed by YFO. Interestingly, the J_c of the tapes with the additions is only large at $H \parallel ab$ but the values of the J_c converge at $H \parallel c$. This is quite unexpected since previous studies have found that Y_2O_3 additions are isotropic pinning centers in PLD-grown [2] and MOD (Metal Organic Deposition)-grown [1] YBCO tapes. Therefore, a decrease in anisotropy and increase in J_c should be found in the whole angular range.

According to STEM data, the YBCO layer of the YFO sample contains dislocations parallel to the *c*-axis such as the areas marked by the horizontal arrows in figure 2a-b. Such dislocations commonly form in MOCVD-grown tapes [7, 8]. We also observe YBCO *a*-axis grains marked by

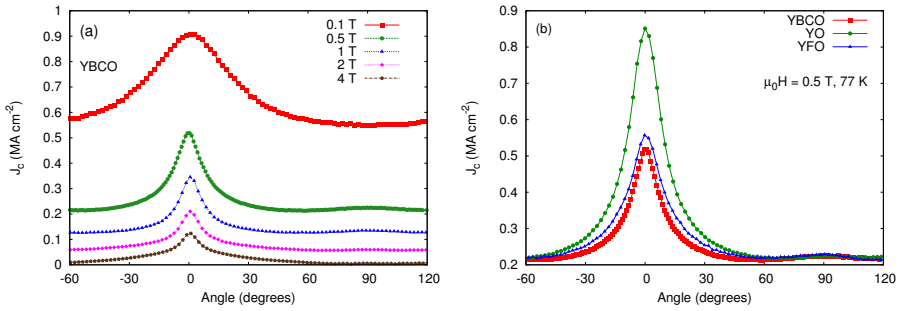

Figure 1. (a) Angular dependence of J_c at 77 K for different fields. (b) Comparison of the three tapes at 0.5 T.

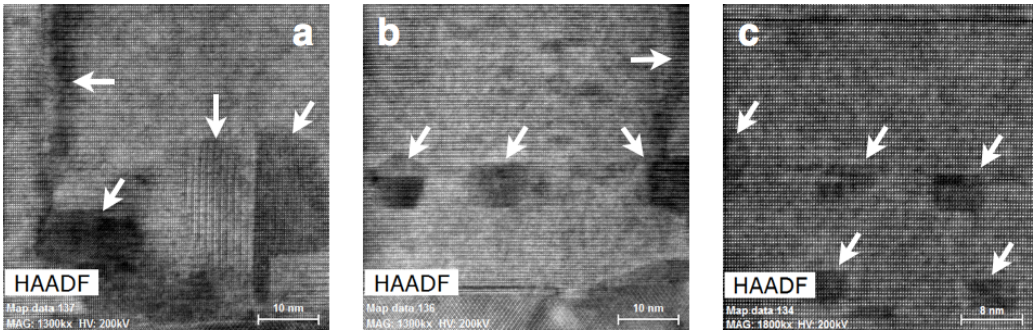

Figure 2. HAADF-STEM images of various parts of the YBCO layer showing dislocations, Y_2O_3 nano precipitates and a-axis grains.

the vertical arrow in figure 2a and Y_2O_3 nanoprecipitates with a diameter of 8-10 nm. Larger particles such as CuO and YCuO grains (100-200 nm in size) were also found by TEM. According to the EDX (Energy-dispersive X-ray spectroscopy) maps, $YFeO_3$ precipitates were not formed but the iron is homogeneously distributed within the YBCO layer and the precipitates consists again of Y_2O_3. This indicates that Cu was partially substituted by Fe in YBCO and the excess Cu formed the CuO and YCuO grains. Therefore, we can deduce that the same type of precipitates is common to YO and YFO tapes and they only vary in amount since the YFO tape contains 1 mol% addition while 10 mol% Y_2O_3 was added to the YO tape.

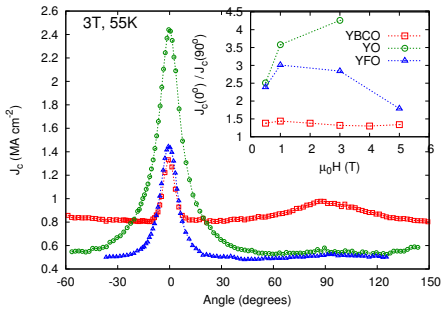

Figure 3. Comparison of $J_c(\theta)$ of the three tapes. The inset shows the ratio of J_c between $H \parallel ab$ and $H \parallel c$.

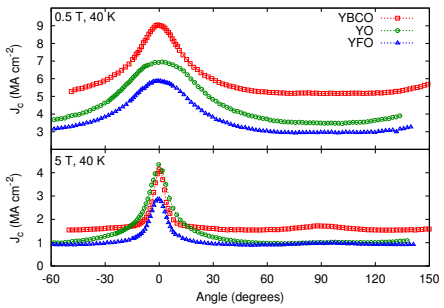

Figure 4. Angular dependence of J_c in the three tapes at 40 K, 0.5 T (top) and 5 T (bottom).

In the measurement at 55 K shown in figure 3, the c-axis peak of the standard YBCO was found to be more prominent than in YO and YFO tapes. We conclude from the TEM data

that the appearance of the c-axis peak may be related to the vortices pinned by the threading dislocations oriented along the c-axis. The standard YBCO was deposited by a two-pass process, however, previous studies showed that the c-axis oriented dislocations are formed continuously over the whole layer thickness in multi-pass processes of the MOCVD technique [8]. The YBCO is also the least anisotropic of the three tapes as shown by the inset in figure 3 in contrary to the unexpectedly strong anisotropy of YFO and YO tapes. The large difference between J_c at $H \parallel ab$ and $H \parallel c$ of the two tapes may be related to the aligned formation of the Y_2O_3 nanoprecipitates parallel to the ab-planes as shown in the TEM image in various parts of the YBCO layer (figure 2b-c). Thus, pinning by these precipitates is strongest along the ab-planes. In $H \parallel c$, only a small section of a vortex is pinned by a precipitate. Also, extra energy arises from the meandering of the vortex lines between the precipitates in other direction not parallel to the ab-planes, thus, pinning is weaker along these directions. The formation of these precipitates is not random in contrast to the precipitates formed by the PLD and MOD techniques. This correlated formation of the nanoparticles was also observed for MOCVD-grown (Y, Sm)$_1$Ba$_2$Cu$_3$O$_y$ films where the (Y, Sm)$_2$O$_3$ particles are arranged in layers and tilted by around 7° from the interface [7, 8]. Although the tilt was not observed in our data, this preferrential formation of precipitates was found to be related to MOCVD deposition process.

The Y_2O_3 nanoprecipitates are no longer effective pinning sites over the whole angular range at 40 K and low fields (3 T and below). The same is also observed at 20 K where $J_c(\theta)$ of YFO and YO tapes is much smaller than in sample YBCO at all fields. Also at this temperature, intrinsic pinning dominates at $H \parallel ab$ in all the tapes, as expected at low temperatures.

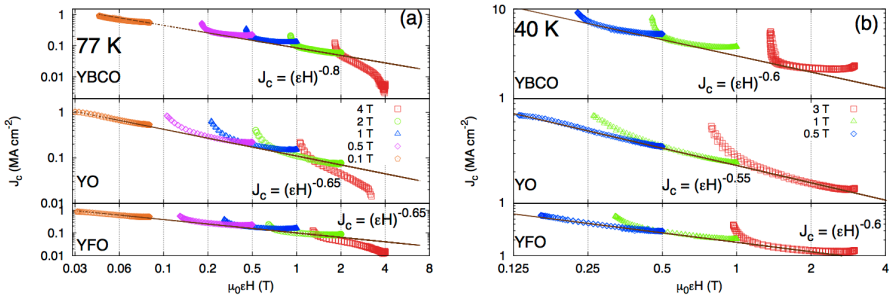

Figure 5. Anisotropic scaling analysis of the three tapes at (a) 77 K and (b) 40 K.

The effective anisotropy γ obtained from anisotropic scaling [9] is 2.2, 3.8 and 3.1 for the standard YBCO, YO and YFO tapes, respectively. The values for γ are smaller than the mass anisotropy in YBCO (γ = 5-7) but close to findings for MOCVD grown tapes [7]. Using $J_c = [\varepsilon(\theta)H]^{-\alpha}$, the determined α decreases at lower temperature. The decrease in α indicates an increase in the density of pinning sites, as smaller defects start to serve as pinning centers when their pinning energy exceeds the thermal energy at low temperature.

4. Conclusion

Y_2O_3 nanoprecipitates were successfully introduced into the YBCO layer of MOCVD grown YBCO tapes with MOCVD-grown (Y, Ce)$O_{1.5+x}$ and CSD-LZO buffer layers on a magnetic Ni5%W substrate. Aside from the Y_2O_3 precipitates, threading dislocations along the c-axis and a-axis grains of YBCO were found by TEM. The Y_2O_3 precipitates contribute to pinning at higher temperatures and hence enhance J_c. However, their effectivity decreases at lower temperatures and lower fields. These precipitates contribute significantly to pinning when $H \parallel ab$ and less for $H \parallel c$. This behavior was attributed to the preferred alignment of the precipitates parallel to ab-planes. Threading dislocations along the direction of the c-axis in

these MOCVD-grown tapes are related to the c-axis peak in $J_c(\theta)$. Intrinsic pinning at $H \parallel ab$ becomes dominant at lower temperature.

Acknowledgment
The research leading to these results has received funding from the European Union Seventh Framework Programme [FP7/2007-2013] under grant agreement n° NMP-LA-2012-280432.

References

[1] Yamasaki H, Yamaguchi I, Sohma M, Kondo W, Matsui H, Manabe T and Kumagai T 2012 *Physica C* **478** 19-28
[2] Mele P, Matsumoto K, Horide T, Ichinose A, Mukaida M, Yoshida Y and Horii S 2007 *Supercond. Sci. Technol.* **20** 616-20
[3] Sparing M, Backen E, Freudenberg T, Hühne R, Rellinghaus B, Schultz L and Holzapfel B 2007 *Supercond. Sci. Technol.* **20** S239-46
[4] Haugan T, Barnes P, Wheeler R, Meisenkothen F and Sumption M 2004 *Nature* **430** 867
[5] Wimbush S, Durrell J, Tsai C, Wang H, Jia Q, Blamire M and MacManus-Driscoll J 2010 *Supercond. Sci. Technol.* **23** 045019
[6] Muydinov R, Stadel O, Falter M and Bäcker M 2012 *Physics Procedia* **36** 1468-74
[7] Chen Z, Kametani F, Chen Y, Xie Y, Selvamanickam V and Larbalestier D 2009 *Supercond. Sci. Technol.* **22** 055013
[8] Holesinger T, Maiorov B, Ugurlu O, Civale L, Chen Y, Xiong X, Xie Y and Selvamanickam V, 2009 *Supercond. Sci. Technol.* **22** 045025
[9] Civale L, Maiorov B, Serquis A, Willis O, Coulter J, Wang H, Jia Q, Arendt P, MacManus-Driscoll J, Maley M and Foltyn S 2004 *Applied Physics Letters* **84** 12
[10] Stadel O, Muydinov R 2009 *IEEE/CSC & ESAS European Superconductivity News Forum (ESNF)* 9